Two-quasiparticle states in ^{250}Cf populated by electron capture decay of 8.6-h ^{250}Es isomer*

M. S. Freedman, I. Ahmad, F. T. Porter, R. K. Sjoblom, R. F. Barnes, J. Lerner, and P. R. Fields
Chemistry Division, Argonne National Laboratory, Argonne, Illinois 60439
(Received 10 September 1976)

The electron capture decay scheme of the 8.6 ± 0.1-h ^{250}Es isomer was investigated with high-resolution γ-ray and β-ray spectrometers and with two parameter coincidence analysis. Mass-separated samples of ^{250}Es produced by ^{249}Bk$(\alpha,3n)$ and ^{249}Cf(d,n) reactions were used for these measurements. We propose a decay scheme involving 32 transitions and 16 levels in ^{250}Cf. In addition to the ground state band, six rotational bands have been identified. The energies (keV) and $K\pi$ values of the bandheads are: 871.67 (2−), 1031.80 (2+), 1255.49 (4−), 1396.18 (5−), 1478.47 (5−), and 1499.62 (6−). The logft values of the electron capture transitions to the four highest bands were deduced and these were used to elucidate the principal two-quasiparticle components of these states. The $K\pi = 2-$ and $2+$ bands were interpreted as octupole and γ-vibrational bands. The following two-quasiparticle configurations have been assigned: 1255.49 (4−), $\{n[734]9/2-;\ n[620]1/2+\}$; 1396.18 (5−), $\{p[633]7/2+;\ p[521]3/2-\}$; 1478.47 (5−), $\{n[734]9/2-;\ n[620]1/2+\}$; and 1499.62 (6−), $\{n[734]9/2-;\ n[622]3/2+\}$. The ground state of the 8.6-h ^{250}Es isomer has been given a spin-parity assignment of 6+ with the configuration $\{n[734]9/2-;\ p[521]3/2-\}$. *KLL* Auger energies and intensities for $Z = 98$ are reported. A K fluorescence yield of 0.976 ± 0.005 is obtained for Cf.

[RADIOACTIVITY ^{250}Es [from ^{249}Bk$(\alpha,3n)$ and ^{249}Cf(d,n); measured $T_{1/2}$, E_γ, I_γ, E_{ce}, I_{ce}, $\gamma\gamma$-coin. ^{250}Cf deduced levels, logft (EC), γ multipolarity, I,π, four two-quasiparticle states, two vibrational states. Mass-separated ^{250}Es. Toroidal β spectrometer at 0.11% resolution (FWHM).]

I. INTRODUCTION

The nuclide ^{250}Es was first discovered by Harvey *et al.*[1] as one of the products of the irradiation of ^{249}Bk with α particles. Its half-life was measured to be 8 h. Recently Ahmad *et al.*[2] observed a 2.1-h ^{250}Es isomer in addition to the 8.3-h isomer in the ^{249}Bk(α,xn) reaction products. From γ-ray spectroscopic measurements they found that the 2.1-h isomer decays mainly by electron capture (EC) to the ground-state band and to the γ-vibrational band at 1031.8 keV in ^{250}Cf. From the logft values a spin-parity of 1− was deduced for the 2.1-h isomeric state.

The electron capture decay of the 8.3-h isomer was found to populate a high spin state (or states) in ^{250}Cf which deexcites to a lower K-value band through low-energy γ rays (140.5, 246.5, 303.2, 349.4, and 383.8 keV). This band, in turn, deexcites to the ground-state band predominantly by 828.8- and 810.1-keV γ rays. From these data and the measured multipolarities of the strong transitions it was deduced that all the observed high-lying states in ^{250}Cf are odd-parity states. However, this work was limited by the small amount of ^{249}Bk available at that time. The recent availability of milligram quantities of ^{249}Bk has prompted us to reinvestigate the ^{250}Es decay scheme in greater detail. Most spectral measurements were started ~10 h after the end of the irradiation and were continued for 2–3 days. For this reason only the decay scheme of the 8.6 h (our present value) isomer has been thoroughly investigated. The present paper describes these measurements and the spin-parity assignments to the states populated in ^{250}Cf.

II. SOURCE PREPARATION

Approximately 2 mg of ^{249}Bk was irradiated with 38-MeV α particles in the Argonne 60-in. cyclotron at an average beam current density of 30 μA/cm^2. The irradiation time varied between 8 and 12 h. The irradiated Bk was dissolved by heating with concentrated HNO_3 and HF. After boiling off the HF, the Bk was dissolved in 10 M HNO_3-0.1 M $KBrO_3$ and extracted with 0.14 F di-(2-ethylhexyl) orthophosphoric acid (HDEHP) in n-heptane.[3] The aqueous phase was equilibrated five times with the HDEHP solution followed by several equilibrations with n-heptane to remove all traces of HDEHP. To the resultant aqueous phase, which contained Es, Cf, and fission products, 1 mg of lanthanum carrier was added and precipitated as hydroxide with NH_4OH. The precipitate was washed once and then dissolved in a minimum amount of HCl and evaporated to dryness. The residue was dissolved in 3 M NH_4CSN-0.01 M H_2SO_4 and loaded on a 2-mm × 6-cm column bed containing Aliquat-336 chloride adsorbed on hydrophobic Celite.[4] After loading, the bed was eluted with 1 M HN_4SCN-0.01 M H_2SO_4. The first

eight free column volumes removed >99.9% of the rare earth fission products and the lanthanum carrier. The Es and Cf were then eluted with 0.02 M H_2SO_4. The H_2SO_4 solution containing the actinides was loaded on a 2.8-mm × 10-cm column bed containing HDEHP adsorbed on hydrophobic Celite. The column was operated at 60°C. A 0.1 M HCl solution was passed through the column which removed most of the remaining fission products. The actinides were then eluted with a 0.5 M HCl solution. The Es was separated from Cf by adsorption on a cation-exchange resin column followed by elution with ammonium α-hydroxy isobutyrate.[5] Isotopically enriched samples of ^{250}Es were then made in the Argonne electromagnetic isotope separator.[6]

A few samples were also produced by the irradiation of ~3 mg of ^{249}Cf with 18-MeV deuterons in the Argonne 60-in. cyclotron. The irradiation and chemical purification procedures have been described elsewhere.[7] The chemically purified einsteinium was run through the isotope separator to prepare thin isotopically enriched sources.

III. EXPERIMENTAL PROCEDURES AND RESULTS

A. γ-ray spectroscopy

Several γ-singles spectra of ^{250}Es samples were measured with high-resolution Ge(Li) spectrometers. The low-energy portion of the spectrum from a mass-separated sample, surveyed with a 2-cm^2 × 0.5-cm planar Ge(Li) diode (resolution 700 eV at 100 keV) is shown in Fig. 1. The run was made ~8 h after irradiation in order to reduce the contribution of the 2.1-h ^{250}Es γ rays and x rays in the spectrum. A 220-mg/cm^2 Al absorber reduced the intensity of L x rays. Au K x rays in the spectrum are due to the fluorescence of the gold electrode on the detector. The $K\alpha_2/K\alpha_1$ intensity ratio was found to be 0.93 ± 0.13, whereas the ratio for pure Au K x rays was measured with the same detector to be 0.59 ± 0.03. This clearly demonstrates the presence of a 67.0-keV γ ray in the Au $K\alpha_2$ peak, verified via its internal conversion L_1 line. The intensity of this γ ray, after subtraction of the Au $K\alpha_2$ intensity, was found to be 0.05 ± 0.02%. The 80.4-keV peak was too wide due to the presence of an 80.0-keV γ-ray component. An enlarged plot of this peak is shown in the inset.

The ^{250}Es γ-singles spectrum was also measured with a 25-cm^3 coaxial Ge(Li) spectrometer. A portion of the spectrum measured with a mass-separated sample is shown in Fig. 2. The spectrum between 400 and 700 keV (not shown) had no γ-ray peaks. Figure 3 shows the spectrum above 700 keV measured with an unseparated ^{250}Es sample. A set of absorbers (0.7-g/cm^2 Pb, 1.0-g/cm^2 Cd, 0.7-g/cm^2 Cu, and 0.5-g/cm^2 Al) attenuated low-energy γ rays and x rays to reduce summing-effect interference. This spectrum was measured ~2 days after the end of the irradiation in order to exclude the 2.1-h γ-ray peaks. The inset spectrum, measured ~8 h after the end of irradiation shows the peaks associated with the decay of the 2.1-h isomer.

The energies and intensities of ^{250}Es γ rays and Cf K x rays obtained from several spectra are summarized in Table I. The errors denote one standard deviation σ. γ rays were assigned to the 8.6-h ^{250}Es on the basis of their decay with the characteristic half-life of ^{250}Es (8.6 h). Intensities, expressed in photons per 100 ^{250}Es (8.6 h) EC decays, were obtained by equating the total

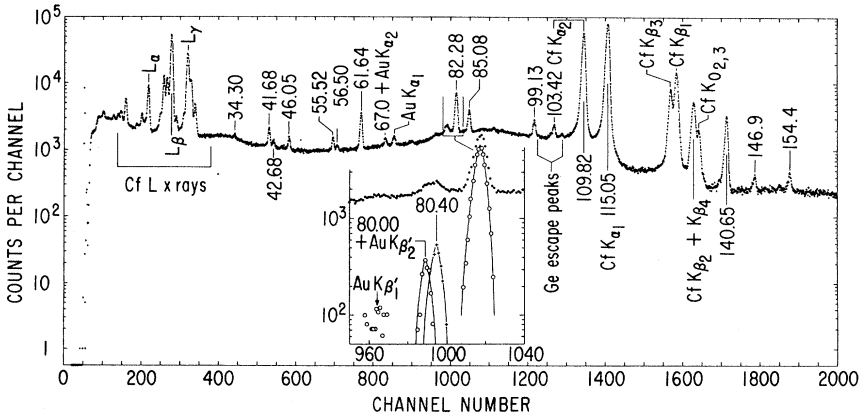

FIG. 1. Low-energy portion of a ^{250}Es (mass-separated) γ-ray spectrum measured through a 350-mg/cm^2 Al absorber with a 2-cm^2 × 5-mm Ge(Li) detector. The inset, which is an enlargement of the 76.6- to 84.2-keV region clearly demonstrates the presence of 80.0- and 80.4-keV peaks. The source was prepared by the ^{249}Cf(d,n) reaction and the spectrum was measured ~8 h after the end of the irradiation. The source was placed ~2 cm from the detector end cap.

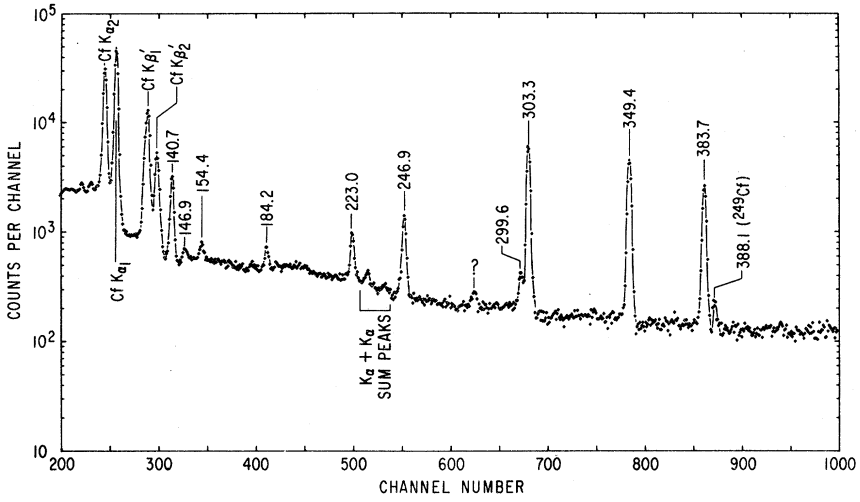

FIG. 2. γ-ray spectrum of a mass-separated ^{250}Es sample measured through a 220-mg/cm^2 Al absorber with a 25-cm^3 coaxial Ge(Li) detector. The source was prepared by the ^{249}Cf(d,n) reaction and the spectrum was measured ~30 h after the end of the irradiation. The source to detector distance was ~10 cm.

γ-ray and conversion-electron intensities populating the ground-state band to 100%, on the assumption of negligible EC feed to this band. Our present γ-ray energies and relative intensities are in excellent agreement with the previous measurements of Ahmad *et al.*[2]

B. Conversion-electron spectroscopy

Instrumentation

The internal conversion lines of the transitions below 141 keV plus a few selected lines of the higher-energy transitions were measured in the Argonne toroidal field spectrometers[8] operated in tandem at instrumental resolutions [full width at half maximum (FWHM)] of 0.18 and 0.11% in momentum with a transmission of ~10%. The sensitivity of our measurement was such that we would have surely detected any electron line in the 5- to 120-keV range with intensity of $\geq$5% per EC decay. Five sources were necessary for this survey because of the 8.6-h half-life. Each of these sources was deposited on 5-mg/cm^2 Al foil in the isotope separator through a 3-mm diameter mask hole.

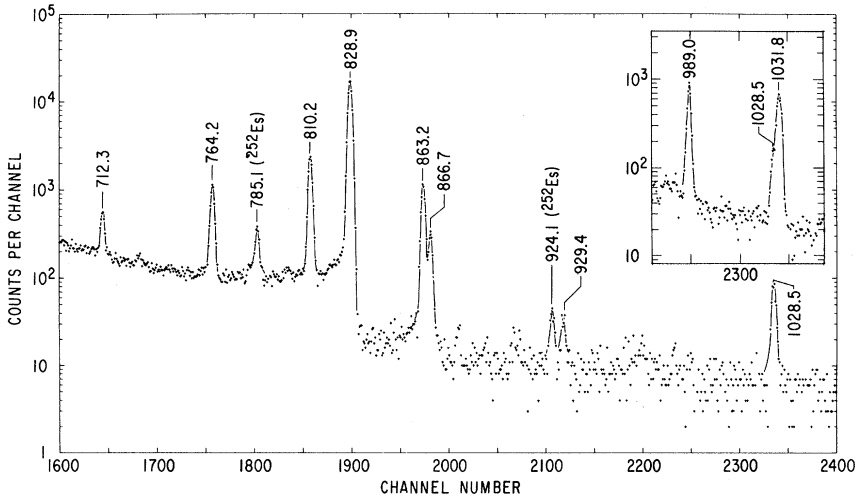

FIG. 3. The ^{250}Es γ-ray spectrum measured with a 25-cm^3 coaxial Ge(Li) detector, ~30 h after the end of the irradiation. The sample was prepared by the ^{249}Bk$(\alpha, 3n)$ reaction and it was not mass-separated. A set of Pb, Cd, Cu, and Al absorbers was used to reduce summing effect interference. The inset spectrum (taken ~9 h after the end of the irradiation) shows the 989.0- and 1031.8-keV peaks which belong to the 2.1-h ^{250}Es isomer.

To reduce electron energy degradation arising from deep ion penetration we collected decelerated ions with energies of 100-200 eV. Source strength at best was 3×10^5 EC dis/min. Estimates of source thickness from upper limits of isotope separator beam current and deposition time yielded ~1 $\mu g/cm^2$.

Line positions were determined from the medians of the upper quarter of peaks. The individual line energy errors (standard deviations) are generated from the position uncertainty and the 60-ppm calibration uncertainty. The atomic electron binding energies used for californium are the result of the electron spectroscopy reported here except the $O_{2,3}$ and $P_{2,3}$ values which are from our own unpublished work on the ^{254}Fm α decay to the 42.721 level in ^{250}Cf. The details of the derivation of the Cf electron binding energies from electron spectroscopy in the ^{250}Es decay will be presented elsewhere.[9]

TABLE I. 8.6-h ^{250}Es γ ray and K x rays.

Energy (keV)	Intensity (photons per 100 ^{250}Es EC decays)	Transition (initial → final state)
34.30 ± 0.06	~0.06	906.0 → 871.7
41.68 ± 0.05	0.29 ± 0.03	1499.6 → 1457.8
42.68 ± 0.05	0.09 ± 0.01	42.7 → 0
46.05 ± 0.05	0.19 ± 0.02	952.1 → 906.0
55.52 ± 0.05	0.20 ± 0.02	1311.1 → 1255.5
56.50 ± 0.05	0.09 ± 0.01	1008.6 → 952.1
61.64 ± 0.05	0.85 ± 0.07	1457.8 → 1396.2
67.0 ± 0.2	0.05 ± 0.02	1377.8 → 1311.1
80.00 ± 0.08	0.11 ± 0.03	1457.8 → 1377.8
80.40 ± 0.05	0.29 ± 0.03	952.1 → 871.7
82.28 ± 0.05	2.6 ± 0.2	1478.5 → 1396.2
85.08 ± 0.05	1.07 ± 0.09	1396.2 → 1311.1
99.13 ± 0.05	0.80 ± 0.07	141.9 → 42.7
103.42 ± 0.05	0.71 ± 0.06	1499.6 → 1396.2
109.82 ± 0.05	46.2 ± 2.3	Cf $K\alpha_2$
115.05 ± 0.05	73.4 ± 3.7	Cf $K\alpha_1$
128.6 ± 0.1 129.8 ± 0.1	30.6 ± 1.5	Cf $K\beta_1'$
133.66 ± 0.1	10.3 ± 0.5	Cf $K\beta_2'$
140.65 ± 0.1	4.7 ± 0.25	1396.2 → 1255.5
146.9 ± 0.1	0.22 ± 0.06	1457.8 → 1311.1
154.4 ± 0.1	0.31 ± 0.06	296.2 → 141.9
184.2 ± 0.2	0.47 ± 0.07	1255.5 → 1071.3
223.0 ± 0.1	1.85 ± 0.13	1478.5 → 1255.5
246.9 ± 0.1	3.8 ± 0.2	1255.5 → 1008.6
299.6 ± 0.2	1.00 ± 0.09	
303.3 ± 0.1	22.3 ± 1.1	1255.5 → 952.1
349.4 ± 0.1	20.4 ± 0.9	1255.5 → 906.0
383.7 ± 0.1	14.0 ± 0.7	1255.5 → 871.7
712.3 ± 0.1	1.34 ± 0.09	1008.6 → 296.2
764.2 ± 0.1	4.0 ± 0.2	906.0 → 141.9
810.2 ± 0.1	9.1 ± 0.5	952.1 → 141.9
828.9 ± 0.1	73.6 ± 3.7	871.7 → 42.7
863.2 ± 0.1	5.1 ± 0.3	906.0 → 42.7
866.7 ± 0.1	1.3 ± 0.1	1008.6 → 141.9
929.4 ± 0.2	0.14 ± 0.02	1071.3 → 141.9
1028.5 ± 0.2	0.45 ± 0.04	1071.3 → 42.7

Intensities of the conversion lines were taken from the line areas (momentum plot). A plot of (peak height/area) vs line energy for the well resolved lines (L and higher shells) is an aid in determining the intensity of weak and poorly resolved lines. Corrections were made for decay (up to four half-lives for the stronger sources) and for detector efficiency. The detector was a bare cleaved-surface NaI(Tl) crystal scintillation counter whose efficiency was obtained from pulse height analysis at several energies. At 7.3 keV the efficiency is 65%, at 14 keV–75%, and at 100 keV–91%. We assign ~10% uncertainty to the counter efficiency correction in the 5–15-keV range. Low-energy lines suffer additional intensity uncertainty because of energy loss phenomena evidenced by a tail on the low-energy side of the line, the extent of which is not always clear. The intensities from different samples and for different resolutions were correlated by running the same line ($L_1 - 82.3$) in each case.

The conversion-electron spectra of ^{250}Es were also measured with a cooled Si(Li) detector[10] mainly to obtain intensities of high-energy transitions not surveyed by the magnetic spectrometer. A portion of the ^{250}Es electron spectrum is shown in Fig. 4. The efficiency geometry of the detector was 1.0% and the resolution (FWHM) was 1.0 keV at 100-keV and 1.6 keV at 600-keV electron energy. The electron intensities were obtained by normalizing at the intensity of the $140.7(L_1+L_2)$ line measured by the magnetic spectrometer. The electron intensities for the $146.8(L_1+L_2)$ line and all conversion electron lines of transitions $\geq$223 keV are given in Table II.

Results: Internal conversion

Table II lists the conversion line data along with γ-ray intensities which are included to get the total intensity for each transition observed for the 8.6-h isomer.[11] The electron and γ-ray intensities were related using 19 well resolved conversion lines from pure $E2$ and nearly pure $M1$ (as determined by subshell ratios) transitions and theoretical conversion coefficients.[12,13] In addition, absolute electron and γ intensities were measured for one of the sources. This absolute comparison resulted in a 10% different normalization than the theoretical conversion coefficient normalization, a result well within the errors of the absolute determinations of the geometries and efficiencies.

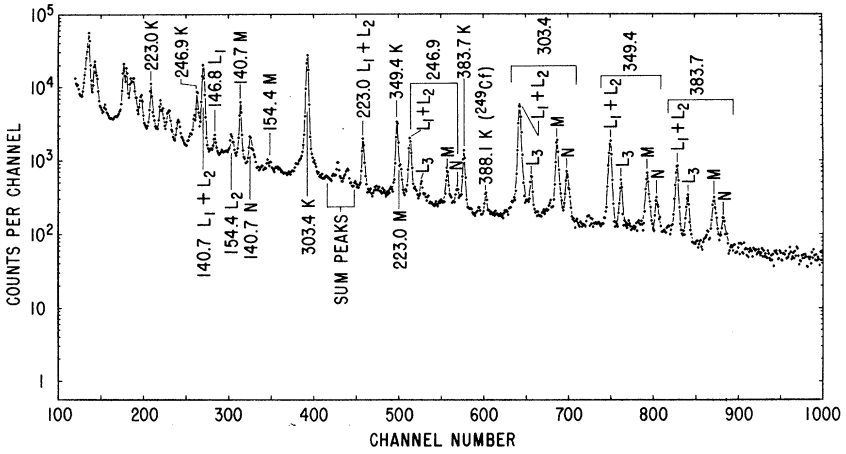

FIG. 4. Conversion-electron spectrum of a mass-separated ^{250}Es sample measured with a cooled Si(Li) detector. The source was prepared by the ^{249}Cf(d,n) reaction and the spectrum was taken ~7 h after the end of the irradiation. The efficiency-geometry product of the detector for electron counts in the peak was 1.0%. The energy scale is 0.437 keV per channel. Low-energy peaks duplicate those taken at better resolution with a magnetic spectrometer.

The intensity errors given in the table include contributions from the line-area and decay-correction uncertainties but none from the counter efficiency correction; these latter errors were omitted because they would lead to overestimates of the errors in the multipole mixing determined from subshell ratios, since the lines involved are not widely spaced in energy and have highly correlated efficiency correction errors.

A measure of the consistency of the intensity data is seen by comparing (see decay scheme, Fig. 5): (1) the intensity of the 42.72-keV transition itself (1.00 in arbitrary units); (2) the intensity feeding the 42.72-keV level (1.01 units); (3) the summed intensity of all transitions to the ground-state band (0.96 units); and (4) the transition intensity out of the 1255.49-keV level (0.99 units). The equality (within 5%) of these numbers is consistent with no electron capture ($\leq 5\%$) to the ground state, 2 −, or 2 + bands. With that assumption each of these is a measure of all the electron capture transitions; we take the average of the four intensities as 100% and quote all intensities relative to that, i.e., % per EC decay.

The γ-plus-conversion-electron intensity into and out of all levels up to 1255.5 keV indicates that electron capture to any of these levels is $\leq 5\%$. The large uncertainty in the intensity of the K line of the 140.7-keV transition makes the deduced intensity of electron capture to the 1255.5-keV and to the 1396.2-keV levels uncertain. This line, shown in Fig. 6, is very broad due to the natural width of the K level (between 130 and 170 eV deduced from this line; about 100 eV expected for $Z = 98$) and the low-energy tailing asymmetry is evident. It is the latter, difficult to measure to lower energy, which gives the large uncertainty to the line intensity. L subshell ratios indicate that the 140.7-keV transition is nearly pure $M1$ (see Table II). If we use theoretical $M1$ conversion coefficient ratios to predict the K intensity, the prediction falls within the experimental limits for the K-140.7 intensity. Using that theoretical value the total 140.7-keV intensity is 75%, and the in-feed (1.06 units) approximately equals the out-feed (0.99 units) at the 1255.5-keV level. This is consistent with the expectation of little electron capture to this level, and in further discussions we take the K-140 intensity to be that given by the theoretical conversion ratios.

In Fig. 7 are shown lines from the weak 102.6- and 103.4-keV transitions intermixed with various other lines. In spite of the complexity, the M_1 and M_2 lines give a measure of the $E2$ mixing in the 103.4-keV transition and verify the $E2$ character of the 102.6 transition, thus providing a basis for the unfolding of the unresolved L lines consistent with theoretical conversion coefficient ratios. When intensities have been partitioned in such a manner for unresolved lines or when the intensity of lines not surveyed is included in the total intensity on the basis of theoretical conversion ratios, the intensities in Table II are in parentheses.

Figure 8 shows the peak at 40.74 keV (4.6015 potentiometer units) which we have assigned to the L_1 conversion of the 67.0-keV transition observed in the γ-ray spectrum. The more accurate energy from the magnetic spectrometer is 66.759 ± 0.010 keV. The L_2 line of this transition was masked by other lines but not the L_3. We found the L_1/L_3 in-

TABLE II. Internal conversion lines in the EC decay of 8.6-h ^{250}Es and total transition intensities.

Transition (Initial → final levels) [keV ±(eV)]	Shell	Energy [keV ±(eV)]	Transition energy [keV ±(eV)]	Intensity[a] (% per decay)	Multipolarity: Data from which derived
34.325(5)	L_1	8.312(5)	34.331(7)	9.4 ±0.8	85% $M1$+
(906.0 →	L_2	9.214(3)	34.325(6)	14.0 ±1.0	(15 ±3)% $E2$
871.7)	L_3	14.419(3)	34.323(7)	(11.7 ±0.8)	M_1/M_2
	M_1	27.566(15)	34.330(16)	1.8 ±0.3	M_1/M_3
	M_2	27.977(8)	34.317(9)	4.1 ±0.3	L_1/L_2
	M_3	29.204(8)	34.322(11)	3.8 ±0.4	
	N_1	32.510(8)	34.326(10)	0.93 ±0.12	
	N_2	32.716(8)	34.326(10)	1.4 ±0.1	
	N_3	33.034(8)	34.323(13)	1.0 ±0.1	
	$O_{1,2,3}$	33.97(63)		0.4 ±0.3	
				48.5 ±2.5	
41.775(5)	L_1	15.754(6)	41.773(8)	18.7 ±4	98% M_1+
(1499.6 →	L_2	16.664(7)	41.775(9)	3.3 ±0.4	(2 ±2)% $E2$
1457.8)	M_1	35.008(9)	41.772(11)	5.1 ±0.5	L_1/L_2
	M_2	35.444(16)	41.784(17)	2.1 ±1.0	M_1/M_2
	N_1	39.959(6)	41.775(8)	1.4 ±.1	
	N_2	40.165(17)	41.775(18)	0.28 ±0.12	
	N_3			≤0.23	
	Other e^-			(3.1)	
	γ		41.68(50)	0.29 ±0.029	
				34.5 ±4	
42.721(5)	L_1	16.731(22)	42.750(22)	1.1 ±0.4	$E2 > 99\%$
(42.7 → 0)	L_2	17.614(3)	42.725(6)	34.6 ±1.7	L_1/L_2
	L_3	22.813(4)	42.717(7)	31.6 ±1.6	
	M_1	35.929(50)	42.693(50)	0.76 ±0.12	
	M_2	36.380(12)	42.720(14)	12.5 ±0.6	
	M_3	37.598(9)	42.716(12)	10.0 ±0.6	
	N_1			(0.15)	
	N_2	41.096(18)	42.706(18)	(3.1 ±0.4)	
	N_3	41.434(10)	42.723(14)	3.2 ±0.2	
	$N_{4,5}$			(0.16)	
	$O_{2,3}$	42.458(35)	42.746(35)	2.0 ±0.3	
	$P_{2,3}$	42.66(100)	42.69(100)	0.7 ±0.3	
	γ		42.68(50)	0.09 ±0.01	
				100.0 ±5	
46.093(5)	L_1	20.075(7)	46.094(9)	8.6 ±0.4	86% $M1$+
(952.1 →	L_2	20.983(7)	46.094(9)	9.1 ±0.7	(14 ±1)% $E2$
906.0)	L_3	26.207(28)	46.111(29)	5.6 ±1.1	L_1/L_2
	M_1	39.334(34)	46.098(34)	2.0 ±0.2	L_1/L_3
	M_2	39.752(7)	46.092(9)	2.5 ±0.2	M_1/M_2
	M_3	40.971(9)	46.089(12)	1.9 ±0.3	
	$M_{4,5}$			(0.05)	
	N_1	44.280(70)	46.096(70)	0.57 ±0.16	
	N_2	44.458(45)	46.068(45)	0.87 ±0.2	
	N_3	44.777(45)	46.066(45)	0.64 ±0.2	
	$O_{1,2,3}$	45.759(45)	46.088(45)	0.74 ±0.2	
	γ		46.05(50)	0.19 ±0.02	
				32.8 ±1.5	
55.602(5)	L_1	29.583(8)	55.602(9)	4.2 ±0.3	74% $M1$+
(1311.1 →	L_2	30.491(8)	55.602(9)	6.8 ±0.4	(26 ±3)% $E2$
1255.5)	L_3	35.726(17)	55.630(18)	(5 ±2)	M_1/M_2

TABLE II (*Continued*).

Transition (Initial → final levels) [keV ± (eV)]	Shell	Energy [keV ± (eV)]	Transition energy [keV ± (eV)]	Intensity[a] (% per decay)	Multipolarity: Data from which derived
	M_1	48.845(11)	55.609(13)	1.25 ±0.2	M_1/M_3
	M_2	49.252(11)	55.592(13)	2.31 ±0.18	
	M_3	50.482(11)	55.600(13)	1.42 ±0.2	
	N_1	53.748(38)	55.564(38)	0.56 ±0.2	
	N_2	53.979(30)	55.589(30)	(0.66)	
	N_3			(0.49)	
	γ		55.52(50)	0.20 ±0.02	
				22.9 ±2	
56.527(13)	L_1			(1.9)	88% $M1$+
(1008.6 →	L_2	31.425(23)	56.536(23)	1.3 ±.3	(12^{+12}_{-5})% $E2$
	L_3	36.638(30)	56.542(30)	0.7 ±0.3	M_1/M_2
952.1)	M_1	49.760(19)	56.524(20)	0.49 ±0.16	
	M_2	50.175(19)	56.515(20)	0.40 ±0.16	
	Other e^-			(0.57)	
	γ		56.50(50)	0.09 ±0.01	
				5.5 ±0.5	
61.667(5)	L_1	35.650(9)	61.669(10)	(20.0 ±1.4)	96% $M1$+
(1457.8 →	L_2	36.554(5)	61.665(7)	5.5 ±0.4	(4 ±1)% $E2$
1396.2)	L_3	41.714(43)	61.618(43)	2.3 ±0.2	L_2/M_1
	M_1	54.898(12)	61.662(13)	5.3 ±0.3	L_1/L_2
	M_2	55.361(20)	61.701(21)	(1.9 ±0.9)	M_1/M_2
	N_1			(1.5)	
	O_1	61.241(41)	61.677(47)	1.1 ±0.5	
	Other e^-			(1.1)	
	γ			0.85 ±0.07	
				39.5 ±2	
66.759(10)	L_1	40.740(9)	66.759(10)	0.6 ±0.1	$M1$+≤20% $E2$
(1377.8 →	L_3			<0.3	L_1/L_3
1311.1)	Other e^-			(0.3–0.9)	
	γ			0.05 ±0.02	
				(1.0–1.9)	
79.998(30)	L_1	53.979(30)	79.998(30)	(1.2 ±0.3)	$M1+E2$
(1457.8 →	L_2			<0.4	L_1/L_2
1377.8)	M_1			<0.6	
	γ			0.11 ±0.03	
				~1.8	
80.412(10)	L_1	54.375(30)	80.394(30)	(0.34)	$E2$
(952.1 →	L_2	55.307(12)	80.418(13)	$(4.7^{+1.5}_{-0.5})$	α_{L_3}
871.7)	L_3	60.501(21)	80.405(22)	4.2 ±0.5	
	M_1			<0.4	
	M_2			(1.43)	
	M_3			1.14 ±0.26	
	Other e^-			(0.7)	
	γ		80.40(50)	0.24 ±0.03	
				12.9 ±1.5	
82.282(6)	L_1	56.264(6)	82.283(8)	27.6 ±1.2	$M1$
(1478.5 →	L_2	57.165(12)	82.276(13)	3.5 ±0.4	($E2 < 0.4$%)
1396.2)	M_1	75.523(14)	82.287(15)	7.2 ±0.4	L_1/L_2
	M_2	75.929(45)	82.269(45)	0.9 ±0.3	
	N_1	80.457(40)	82.273(40)	2.0 ±0.5	
	O_1	81.843(24)	82.279(35)	0.56	

TABLE II (*Continued*).

Transition (Initial → final levels) [keV ± (eV)]	Shell	Energy [keV ± (eV)]	Transition energy [keV ± (eV)]	Intensity [a] (% per decay)	Multipolarity: Data from which derived
	O_2	81.923(24)	8.252(25)		
	Other e^-			(0.6)	
	γ		82.24(50)	2.6 ±0.2	
				45.0 ±2	
85.086(7)	L_1	59.061(12)	85.080(13)	10.0 ±0.5	M_1+
(1396.2 →	L_2			(1.8 ±0.3)	($E2 \leq 7\%$)
1311.1)	L_3	65.283(84)	85.187(84)	0.5 ±0.5	L_1/L_3
	M_1	78.323(9)	85.087(11)	(2.3 ±0.2)	
	M_2	78.749(13)	85.089(14)	0.59 ±0.07	
	N_1	93.274(24)	85.090(25)	0.86 ±0.15	
	Other e^-			(0.37)	
	γ		85.08	1.07 ±0.09	
				17.5 ±1	
99.160(10)	L_1	73.225(66)	99.244(66)	0.8 ±0.3	$E2 > 90\%$
(141.9 →	L_2	74.055(11)	99.166(12)	(8.1 ±0.5)	L_1/L_3
42.7)	L_3	79.249(14)	99.153(15)	5.3 ±0.3	
	M_2	92.813(16)	99.153(17)	2.4 ±0.2	
	M_3	94.032(16)	99.150(17)	1.7 ±0.2	
	N_2			(0.81)	
	N_3	98.886(26)	99.175(26)	0.47 ±0.06	
	Other e^-			(0.6)	
	γ			0.80 ±0.07	
				21.0 ±1	
102.623(10)	L_1	76.616(45)	102.635(45)	0.13 ±0.13	$E2 > 94\%$
(1008.6 →	L_2	77.522(23)	102.633(24)	(1.5 ±0.3)	M_1/M_2
906.0)	L_3	82.718(12)	102.622(13)	1.09 ±0.15	
	M_1			<0.05	
	M_2	96.280(15)	102.620(16)	0.51 ±0.04	
	M_3			(0.29)	
	Other e^-			(0.3)	
	γ			(~0.2)	
				4.0 ± 0.4	
103.440(10)	L_1	77.426(17)	103.445(18)	(3.8 ±0.3)	94% $M1$+
(1499.6 →	L_2	78.323(9)	103.434(10)	(1.1 ±0.2)	(6 ±5)% $E2$
1396.2)	M_1	96.685(15)	103.449(16)	0.99 ±0.06	M_1/M_2
	M_2	97.124(50)	103.464(50)	0.25 ±0.06	
	Other e^-			(0.3)	
	γ		103.42(50)	0.71 ±0.06	
				7.2 ±0.7	
140.694(10)	K	5.722(7)	140.693(15)	(55.0) [b]	$M1$
(1396.2 →	L_1	114.669(15)	140.688(16)	10.4 ±0.4	(<1% $E2$)
1255.5)	L_2	115.591(18)	140.702(19)	1.41 ±0.06	L_1/L_2
	L_3			(0.1)	
	M_1	133.937(58)	140.701(58)	2.8 ±.4	
	M_2			(0.4)	
	Other e^-			(1.1)	
	γ			4.7 ±0.3	
				75^{+5}_{-20}	

TABLE II (*Continued*).

Transition (Initial → final levels) [keV ±(eV)]	Shell	Energy [keV ±(eV)]	Transition energy [keV ±(eV)]	Intensity[a] (% per decay)	Multipolarity: Data from which derived
154.349(60 (296.2 → 141.9)	L_2	129.213(70)	154.324(70)	0.79 ±0.08	$E2$
	L_3			(0.39)	α_{L_2}
	Other e^-			(0.57)	
	γ		154.40(100)	0.31 ±0.07	
				2.1 ±0.2	
146.8(100)[c] (1457.8 → 1311.1)	L_1	120.8(100)	146.8(100)	0.50 ±0.05	$M1$
	L_3			<0.05	<25% $E2$
	Other e^-			(2.50)	α_{L_3}
	γ			0.22 ±0.06	
				3.2 ±0.3	
222.993(20) (1478.5 → 1255.5)	K	88.022(10)	222.993(20)	5.20 ±0.21	$M1$+
	L_1+L_2			1.10 ±0.06	(15 ±4)% $E2$
	L_3			≤0.05	α_K
	M			0.33 ±0.02	
	$N+0+\cdots$			(0.12)	
	γ			1.85 ±0.13	
				8.6 ±0.3	
246.921(55) (1255.5 → 1008.6)	K	111.950(53)	246.921(55)	4.92 ±0.25	$M1$+
	L_1+L_2			1.45 ±0.07	(50 ±3)% $E2$
	L_3			0.13 ±0.017	α_K
	M			0.40 ±0.03	
	$N+0+\cdots$			(0.15)	
	γ			3.8 ±0.2	
				10.7 ±0.4	
303.409(30) (1255.5 → 952.1)	K	168.438(23)	303.409(30)	17.6 ±0.9	$M1$+
	L_1+L_2			4.7 ±0.24	(54 ±3)% $E2$
	L_3			0.30 ±0.02	α_K
	M			1.30 ±0.07	
	$N+0+\cdots$			0.47 ±0.03	
	γ			22.3 ±1.1	
				46.7 ±1.6	
349.4 (1255.5 → 906.0)	K			2.15 ±0.13	$E2$+
	L_1+L_2			1.48 ±0.07	(4.5 ±0.8)% $M1$
	L_3			0.28 ±0.02	α_K
	M			0.50 ±0.03	
	$N+0+\cdots$			0.18 ±0.015	
	γ			20.4 ±0.9	
				25.0 ±1.0	
383.7 (1255.5 → 871.7)	K			0.80 ±0.04	$E2$
	L_1+L_2			0.70 ±0.04	<0.6% $M1$
	L_3			0.15 ±0.013	α_K
	M			0.24 ±0.017	
	$N+0+\cdots$			0.10 ±0.012	
	γ			14.0 ±0.7	
				16.0 ±0.8	
764.2 (906.0 → 141.9)	K			~0.03	$E1$; α_K
	γ			4.0 ±0.2	

TABLE II (*Continued*).

Transition (Initial→ final levels) [keV ±(eV)]	Shell	Energy [keV ±(eV)]	Transition energy [keV ±(eV)]	Intensity[a] (% per decay)	Multipolarity: Data from which derived
810.2	K			0.045 ±0.007	$E1$; α_K
(952.1→	γ			9.1 ±0.5	
141.9)					
829.00(70)	K	694.13(70)	829.10(70)	0.39 ±0.03	$E1$
(871.7→	L_1+L_2			0.082 ±0.007	<0.3% $M2$
42.7)	M			0.028 ±0.004	α_K
	γ			73.6 ±4.0	
				74.1 ±4.0	
863.2	K			~0.02	$E1$; α_K
(906.0→	γ			5.1 ±0.3	
42.7)					

[a] Intensities in parentheses for unobserved or incompletely resolved lines are calculated from the measured transition multipolarity admixture.

[b] Observed intensity of this low-energy line lies between 35% and 60% per EC decay. The number in the table is that predicted by theoretical conversion ratios which we judge to be the best value to use for decay scheme intensity analysis. The error given for the transition intensity refers to the experimental uncertainty for the K line.

[c] Intensities of all transitions ≥146.9 keV (except 154.4 keV), reported in this table, were measured with a cooled Si(Li) detector. Transition energies with errors represent magnetic spectrometer values; transition energies without errors given in column 1 only denote γ-ray energies measured with Ge(Li) spectrometers.

tensity ratio > 2 which indicates a predominantly $M1$ character for the 67.0-keV transition.

In Table II we indicate evidence for the L_1 line of a 79.99 ± 0.03-keV transition which has very nearly the same electron energy as the N_2-55.602 line. Theoretical conversion coefficients suggest that ~$\frac{2}{3}$ of the line intensity cannot belong to the N_2-55.602 line and hence we have assigned that portion of the intensity to the L_1-79.99 line. An 80.0-keV γ ray has been identified in the photon spectrum.

Of the approximately 100 conversion lines observed (not including the 50 L Auger line spectrum to be reported elsewhere) there is only one which has uncertain assignment. The line is at 5.522 keV (~5% per decay) on the low-energy side of the K-140.7 peak (see Fig. 6). This is very close to the $L_1L_3N_6$ and $L_1L_3N_7$ Coster-Kronig (CK) lines calculated to be at 5.507 and 5.531 keV on a $Z+1$ assumption for N electron binding in the L^{-1} hole state. Its intensity is about half that predicted for the assumed CK lines by McGuire's calculation[14] using the primary L_1 vacancies (144% per decay) deduced from our decay data. Also possible at this energy value is a $M_2O_1O_2$ Auger line but the assignment is unlikely since there is no $M_2O_1O_3$ just 90 eV higher in energy. No attempt was made to survey the L Coster-Kronig or M Auger regions systematically.

Results: KLL Auger transitions

Table III gives the measured and theoretical[15,16] energies and intensities of the KLL Auger lines in Cf indicating agreement for each in all cases. The bottom line gives the ratio of KLL events to the total K holes as calculated from theoretical K/total capture ratios[17] and from the measured total K conversion intensity. Assuming[18] [K Auger (total)/KLL] − 1 = 0.7 ± 0.2 one obtains a fluorescence yield for the K shell in californium of (97.6 ± 0.5)%.

The total K holes calculated were 160% per decay compared to (164 ± 7)% per decay obtained from the measured K x-ray intensity (Table I) and the fluorescence yield.

C. Two-parameter γ-γ coincidence measurements

A γ-γ coincidence experiment using a multiparameter analyzer was performed. The γ rays were detected with 4-cm^3 and 25-cm^3 Ge(Li) diodes using a resolving time (2τ) of 2 μs. Coincidence events were accumulated on magnetic tape which were later read back into the analyzer memory through a digital gate system. In this way the γ-ray spectrum above the K x rays in coincidence with selected photopeaks (used as gates) was obtained. The results are summarized in Table IV. The weaker γ rays (e.g., γ rays below 110 keV

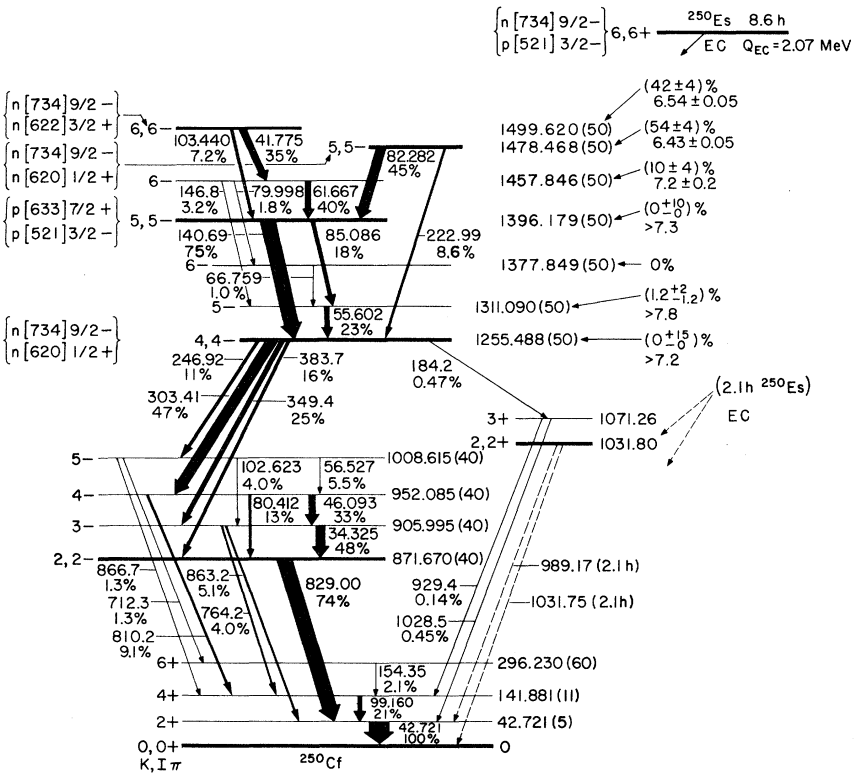

FIG. 5. Level diagram of ^{250}Cf constructed on the basis of the present investigation. Transition intensities in ^{250}Cf in percent per ^{250}Es (8.6 h) EC decay are given below transition energies in keV. Intraband transitions are shown by vertical arrows; the interband transitions by slanted arrows. The EC intensities shown in the figure are derived from transition intensity balances; log*ft* values are shown below EC intensities. Level energies are given in keV (± eV). $K, I\pi$, and Nilsson state configurations of the bands are shown on the left side of levels; K for bandheads only.

and the 223.0-keV γ ray) were not intense enough to be identified in the coincidence spectrum. Thus their absence in Table IV does not necessarily imply no cascade with the particular γ ray listed as gate. All coincidence results are consistent with the decay scheme shown in Fig. 5.

D. Half-life

The half-life of the ^{250}Es nuclide was measured as 8.6±0.1 h by following the decay of the 349.4-keV γ ray on a mass-separated sample with a 25-cm^3 Ge(Li) spectrometer. In addition the half-life of the L_1-82.28 line observed in the magnetic spectrometer was 8.6±0.2 h.

IV. DECAY SCHEME ANALYSIS

A. General

The construction of the decay scheme was based on energy and intensity balances, the aforementioned coincidence results, and multipolarity data, as will be detailed with respect to particular levels. For the assignments of transitions, partic-

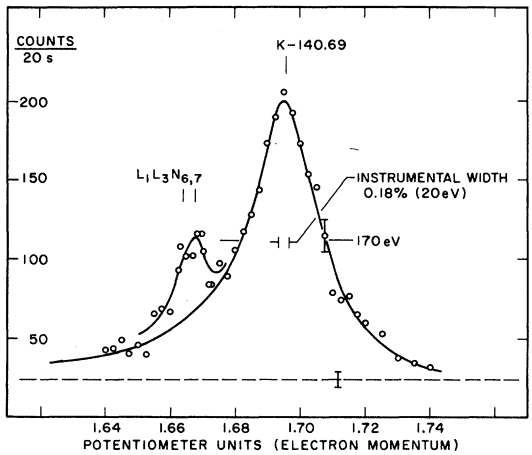

FIG. 6. The 5.718-keV K conversion-electron line of the 140.694-keV transition measured with the magnetic spectrometer. Large uncertainty in the intensity of this transition arises from the extent of the low-energy tail. The line at 1.667 potentiometer units (5.522 keV) has been tentatively assigned as an $L_1L_3N_{6,7}$ Coster-Kronig line. The error bar beneath the line indicates uncertainty in the background.

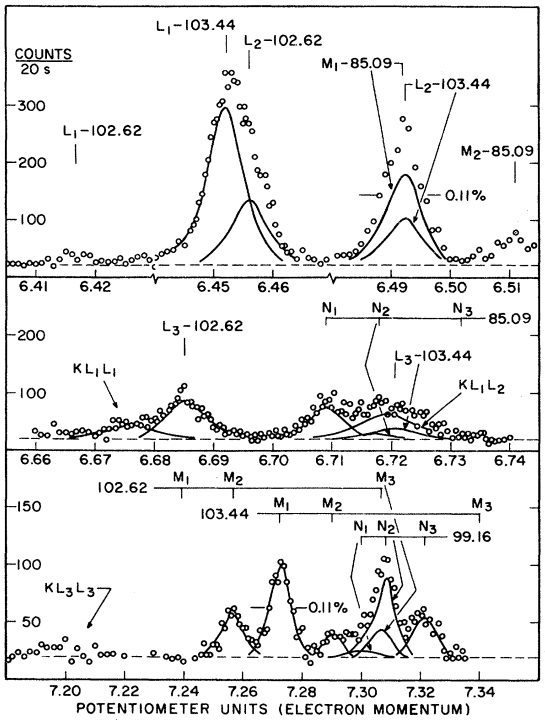

FIG. 7. Internal conversion lines in the 8.6-h ^{250}Es→^{250}Cf decay showing the complex L and M regions of the 103.44- and 102.62-keV transitions. Labels with vertical marks show the expected positions of the lines. Even though the 103.44 L lines are unresolved from neighbors at this resolution, the M_1/M_2 ratio gives the $M1$-$E2$ multipole mixing and hence, with theoretical conversion coefficient ratios, the intensities of the 103.44 L lines. Such unfoldings based on theoretical conversion coefficient ratios are drawn in as solid lines under the experimental points. The KL_1L_1 and KL_1L_2 intensities are the residues after the expected line intensities were subtracted. They have ~35% broader line widths than L and M conversion lines at the same energy because of the natural width of the K level.

ularly those of low energy within a band, the precision of energy determination by electron spectroscopy made the identification of crossover-stopover triplets essentially unambiguous; no stopover sum-crossover disparity exceeded 6 eV within a band, or 40 eV between bands.

Best values for the level energies in ^{250}Cf are given in the decay scheme (Fig. 5). Note that within bands other than the ground-state band the level separations are better known than the assigned errors would indicate. These larger errors reflect the uncertainty in values of the high-energy transitions connecting the bands. For example all the members of the 2− band have a correlated 40-eV uncertainty derived from the six high-energy transitions connecting it to the ground-state band whereas the interband spacings are known to 5–15

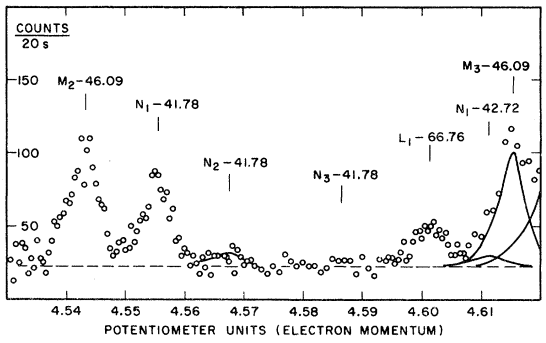

FIG. 8. Conversion electrons from the 8.6-h ^{250}Es→^{250}Cf decay. Labels with vertical marks show expected positions of lines. Note the weak L_1 conversion line of the 66.76-keV transition. Its L_2 line is masked by other lines (not shown) but support for this assignment is found in the photon spectrum.

eV.

Only one weak (≲2% per decay) 299.6-keV transition could not be unambiguously placed in the scheme.

The EC feed to any level was determined by subtracting the total $\gamma+e^-$ intensity (% per decay) populating that level from the total $\gamma+e^-$ intensity deexciting that state. Logft values (Fig. 5) were determined using a value[19] of 2.07 MeV as the 8.6-h ^{250}Es EC decay energy.

B. Ground-state band

The energies of the rotational members of the ground-state band are known from the α-decay studies[20] of ^{254}Fm and β-decay studies[21] of ^{250}Bk. In the present work the energies of the 2+, 4+, and 6+ members of the ground-state band have been measured very accurately. The multipolarities of the lower two transitions in the band are found to be >90% $E2$ (see Table II). The rotational energies of the members of the ground-state band can be calculated from the equation[22]

$$E_I = AI(I+1) + BI^2(I+1)^2 , \quad (1)$$

where I is the nuclear spin of the state, A $(=\hbar^2/2\mathcal{I})$ is the rotational constant, and B is a constant which is a measure of the rotation-vibration coupling. From the 2+ and 4+ energies the values of A and B are calculated to be 7.1314 ± 0.0009 keV and −(1.87 ± 0.07) eV, respectively. The energy of the 6+ state is calculated to be 296.22 ± 0.13 keV which is in excellent agreement with the experimental value of 296.23 ± 0.06 keV.

The energy balances among the high-energy transitions 712, 764, 810, 829, 863, and 867 keV, and the low-energy crossover-stopover groups 80, 34, 46, 102, and 56 keV determine the existence

TABLE III. *KLL* Auger lines observed in the 8.6-h ^{250}Es→^{250}Cf decay. $\sum KLL/\sum K$ holes $= 0.014 \pm 0.002$.

Lines ($Z=98$)	Energy (keV)	Energy (theory[a])	Intensity (% per decay)	Intensity (theory[b])
KL_1L_1	82.49 ±0.07	82.585	0.4 ±0.1	0.45
$KL_1L_2(^1P_1+{}^3P_0)$	83.51 ±0.07	83.519	0.9 ±0.2	0.90 (norm)
$KL_1L_3(^3P_1+{}^3P_2)$	88.65 ±0.05	88.672	0.4 ±0.1	0.28
KL_2L_3	89.58 ±0.03	89.573	0.45 ±0.08	0.39
$KL_3L_3(^3P_0+{}^3P_2)$	94.8 ±0.1	94.775	0.18 ±0.09	0.13
KL_2L_2				0.03
			2.3 ±0.3	

[a] Reevaluated from the tables of Larkins (Ref. 15) using binding energies from a semi-empirical evaluation (Ref. 9) for $Z=84$–103 instead of earlier binding energy values from K. D. Sevier [*Low Energy Electron Spectroscopy*, (Wiley Interscience, New York, 1972)] used by Larkins.

[b] Reference 16; extrapolated to $Z=98$ and normalized to the experimental intensity for KL_1L_2.

of a bandhead level at 871.67 keV with certainty, as well as the levels in the ground-state band terminating the high-energy transitions. The intensity balances within the ground-state band indicate that essentially all its population comes via the high-energy γ rays, and that no direct electron capture takes place to this band. This same conclusion applies to the band based on the 871-keV level ($K\pi = 2-$, details below). Both observations suggest a high spin for the 8.6-h ^{250}Es isomer.

The 2.1-h isomer, on the other hand, is known[2] to decay directly by EC to the ground-state band with substantial intensity ($\log ft = 6.7$), indicating that it is a low spin isomer; 1− was proposed[2] for its spin-parity.

C. Configuration of the ^{250}Es isomer

We digress to present the evidence for the spin-parity assignment for the parent Es isomer. To establish the spin-parity of the 8.6-h (and 2.1-h) isomers we consider all possible neutron-proton couplings based on single-particle states lying within ~ 200 keV of the Fermi level in nearby odd-A nuclei. The ground state of ^{249}Cf is known to be a $\frac{9}{2}-[734]$ neutron orbital from the α-decay studies[23,24] of ^{249}Cf and ^{253}Fm. (The only other available neutron state, $\frac{5}{2}+[622]$, lies[24] 145 keV above this $\frac{9}{2}-$ state in ^{249}Cf. For reasons to be described below we reject this state as the neutron component for the 8.6-h ^{250}Es isomer.) The ground states of the known Es isotopes ($Z=99$) have been given the following proton state assignments: ^{249}Es, $\frac{7}{2}+[633]$ (Ref. 7); ^{251}Es, $\frac{3}{2}-[521]$ (Ref. 2); ^{253}Es, $\frac{7}{2}+[633]$ (Ref. 25). Hence preferred candidates for the spin-parity of the 8.6-h and 2.1-h ^{250}Es isomers are 1−, 8−, 3+, or 6+ formed by the coupling of the $\frac{9}{2}-[734]$ neutron orbital with these proton states. The 2.1-h isomer preempts the 1− state, as indicated. The lack of known isomeric transition between the ^{250}Es states (it is not known which is the upper), together with the low electron capture probability of the 8.6-h isomer to the ^{250}Cf ground-state band, to the $K=2-$ band (head at 871.7 keV) or to the $K=2+$ band (head at 1032 keV), rule out the 3+ spin-parity assignment. The 8− assignment is inconsistent with the low $\log ft$ values to the 1478- or 1396-keV levels, whose spins cannot exceed 5− (see below). Thus the 8.6-h ^{250}Es isomer is assigned spin-parity 6+, with the configuration $n[734]\frac{9}{2}-$; $p[521]\frac{3}{2}-$.

We indicate the arguments rejecting the $\frac{5}{2}+[622]$ neutron component for the 8.6-h ^{250}Es state. The spin-parity states generated by coupling this neu-

TABLE IV. Summary of two-parameter γ-γ coincidences.

Gate	γ rays (keV)
$K\alpha$ x rays	K x rays, 140.7, 184.2, 223.0, 246.9, 299.6, 303.3, 349.4, 383.7, 712.3, 764.2, 810.2, 828.9, 863.2, 866.7
140.7	K x rays, 246.9, 303.3, 349.4, 383.7, 764.2, 810.2, 828.9, and 863.2
303.3	K x rays, 140.7, 764.2, 810.2, 828.9, 863.2
349.4	K x rays, 140.7, 764.2, 828.9, and 863.2
383.7	K x rays, 140.7, 828.9
764.2	K x rays, 140.7, 303.3, and 349.4
810.2	K x rays, 140.7 and 303.3
828.9	K x rays, 140.7, 246.9, 303.3, 349.4, and 383.7
863.2	K x rays, 140.7, 303.3, and 349.4

tron state with the $\frac{7}{2}+$ and $\frac{3}{2}-$ proton states are 1+, 6+, 1−, and 4−. Only the 6+ and 4− states need be considered for the 8.6-h isomer. For each of these possibilities, we tested all sets of four two-quasiparticle state assignments (for the four bandheads in ^{250}Cf above 1200 keV), given by the calculations of Soloviev and Siklos[26] for ^{250}Cf in this energy range. No such set either contained at least two two-quasiparticle states which could be fed by single-particle electron-capture transitions from either of these 6+ or 4− ^{250}Es states (needed to account for the intense capture branches to two high bands of Fig. 5) or else did so only at the expense of at least 0.5-MeV inversion of the level order predicted by Soloviev and Siklos.[26]

D. Collective bands in ^{250}Cf

We resume the discussion of the ^{250}Cf levels. The measured $E1$ multipolarity of the 829.0-keV transition ($\alpha_K E2 = 0.016$; $\alpha_K E1 = 0.0053$; $\alpha_K M2 = 0.185$; α_K exp $= 0.0053 \pm 0.0005$) limits the spin-parity of the 871.67-keV level to 1−, 2−, and 3− only. The fact that no γ-ray branching to the 0+ or 4+ member of the ground-state band is observed strongly favors a 2− assignment. This assignment is further supported by the alternating pattern of single and double interband γ rays deexciting the members of the 871.67-keV 2− collective band (see Sec. IV F).

The energy levels in a 2− band can be represented by[27]

$$E_I = AI(I+1) + BI^2(I+1)^2 + CI^3(I+1)^3 + B_4(-1)^I(I-1)I(I+1)(I+2), \quad (2)$$

where the B_4 contribution, which alternates in sign with level spin, is applicable in this case with $K=2$. Theoretical estimates[27,28] of C and B_4 indicate that contributions from both these terms are large compared to the measured energy uncertainties.

We fitted Eq. (2) to the three level differences of the 2− band with the coefficient $C=0$ (the ratio $C/B = 0.01$ was found[29] for the 2− band in ^{234}U), and obtained $A = 5.742$ keV, $B = -0.45$ eV, and $B_4 = 0.56$ eV. A plot of the quantity

$$A_{I+1,I} = E_{I+1,I}/[(I+1)(I+2) - I(I+1)] = \tfrac{1}{2}E_{I+1,I}(I+1)$$

derived from the energy spacing $E_{I+1,I}$ between the levels of spin $I+1$ and I for the first three level spacings in the 2− band, vs $(I+1)^2$, shows the start of a possible B_4-generated sawtooth behavior with B_4 positive, i.e., $A_{4,3}$ greater than both $A_{3,2}$ and $A_{5,4}$. This behavior indicates an interaction in which the odd-spin states are depressed with respect to the even-spin states; just the reverse was found for the 2− band in ^{234}U by Bjørnholm *et al.*[29] ($A_{4,3}$ less than both $A_{3,2}$ and $A_{5,4}$, i.e., B_4 negative). The effect in the case of ^{234}U was ascribed to the repelling (raising) effect on the odd-spin members of the 2− band by a 0− band (I = only 1, 3, 5) ~ 180 keV *below* the 2− band. A similar 0− band, but ~ 240 keV *above* the 2− band in ^{250}Cf, suggested by Meyer *et al.*[30] from the ^{250}Bk decay data, may be the origin of the observed depression of the spin 3 member in our case. The ratio $|(A_{4,3} - A_{5,4})|/|(A_{4,3} - A_{3,2})|$ is ~30% smaller for ^{250}Cf than for ^{234}U, in agreement with this interpretation.

The $2+\gamma$ vibrational band based on the 1031.8-keV level is well established[21] in the decay of ^{250}Bk. It is strongly populated in the EC decay[2] of the 2.1-h ^{250}Es isomer. In the 8.6-h decay only its first rotational (3+) level is fed significantly, almost solely by the weak 184.2-keV γ ray. We observe only the high-energy deexciting γ rays of the 3+ state persisting after the 1031.8- and 989.0-keV γ rays from the 1031.8-keV level have decayed with a 2.1-h half-life. A small branch of the 2.1-h decay does go through the 2− band as evidenced by a 2.1-h component in the 829.0-keV transition. Because the interband transitions from the 2+ to 2− states are not obvious it is assumed that there is a small amount of capture from the 2.1-h isomer to the 2− band.

E. Higher intrinsic excitation states

The energy and intensity balances of the 184-, 247-, 303-, 349-, and 384-keV transitions and the coincidence relationships establish a level at 1255.5 keV. The multipolarities of the transitions connecting this state to the 2− band uniquely determine the spin-parity of the 1255.5-keV state as 4−. From the 140.694- (85.086 + 55.602) keV energy balance and the relative intensities we order the 85.09- and 55.60-keV transitions as shown. The $M1$ multipolarity of the 55.60-keV transition and the agreement with the expected 4− 5 rotational spacing (see Sec. IV G) make the 1311.1-keV level the $I=5$ member of the $K=4$ band. From the 146.8- (66.76 + 80.00) keV energy balance we place a level at 1377.8 keV and because of $M1$ multipolarities of these transitions we interpret it as the 6− member of the $K\pi = 4-$ band at 1255.5 keV; its energy fits well as the 6− state.

The observed coincidence of the 140.69-keV γ ray with the 383.7- and 829.0-keV γ rays together with the high relative intensity of the 140.69-keV transition establishes a level at 1396.2 keV. The $M1$ character of the 140.69- and 85.09-keV transitions limits the spin-parity of the 1396.2-keV state to 4− or 5−. It is given a 5− assignment for reasons presented in Sec. IV F based on electron

capture intensities populating high-energy levels. Because the 1396.2-keV level deexcites predominantly to the $K=4-$ band, it is interpreted as a bandhead level with $K=5$. If the 1396.2-keV level were not a bandhead, strong intraband transitions to lower-spin members would be expected. The $M1$ multipolarities of the 146.9-, 80.00-, and 61.67-keV transitions establish a level at 1457.8 keV with spin-parity of 5 – or 6 –. We assign the 1457.8-keV level to the 6– member of the $K\pi=5-$ band at 1396.2 keV because this level spacing gives a reasonable value of the rotational constant (5.13 keV).

Energy balances indicate a level at 1478.5 keV and the $M1$ multipolarities of the 82.28- and 223.0-keV transitions restrict its spin-parity to 4 – and 5 –. The low logft value of 6.4 to this state rules out the possibility of spin 4 and hence we give a $K, I\pi = 5, 5-$ assignment to the 1478.5-keV state. Its assignment as a bandhead follows from the absence of a strong ~56-keV transition to a 4– member of the band; moreover, a second 4– band is not expected near this excitation energy.

The level at 1499.6 keV is established from the 103.44- (41.78+61.67) keV energy balance. The $M1$ multipolarities of the transitions connecting this level to the lower 5– and 6– states restrict its spin-parity to 5 – and 6 –. It is given a $K, I\pi = 6, 6-$ assignment on the basis of arguments to be given in Sec. IV F. The order of the 41.78- and 61.67-keV transitions follows from the independently established level at 1457.8 keV and is consistent with the greater intensity of the 61.67 keV transition.

The existence of all the levels in ^{250}Cf observed in the ^{250}Es decay is also confirmed by nuclear reaction studies[31] as discussed in the following section.

F. Two-quasiparticle Nilsson state configurations

The EC transitions in odd-odd nuclei, in which one nucleon necessarily remains in the same orbital in the parent and daughter (the β decay operator can change only one orbital), are analogous to EC decays in nearby odd-A nuclei involving the same single-particle states. In our comparison of logft values in the 8.6-h ^{250}Es decay with those in such odd-A nuclei we have ignored the corrections due to pair correlation effect and the effects of differences of odd-A and even-A initial and final state spins. Since the ground state of ^{250}Es has the configuration $\{n[734]\,\frac{9}{2}-;\ p[521]\,\frac{3}{2}-\}_{6+}$, the two-quasiparticle states fed in the EC decay must contain either of these orbitals. Such two-quasiparticle states in ^{250}Cf can be generated from the single-particle spectra in the neighboring odd-n states of ^{249}Cf (Refs. 7 and 24) and ^{251}Cf (Ref. 32) and odd-p states of ^{249}Bk (Ref. 33). The transitions $p[521]\,\frac{3}{2}- \rightarrow n[620]\,\frac{1}{2}+$ and $p[521]\,\frac{3}{2}- \rightarrow n[622]\,\frac{3}{2}+$ are known in the EC decay[2] of ^{251}Es with logft values of 6.2 and ~5.7, respectively. A β transition in ^{249}Bk with a logft value of 7.1 connects the $p[633]\,\frac{7}{2}+$ and $n[734]\,\frac{9}{2}-$ states.[21] These known single-particle states, plus the predictions of the 1964 calculations of Soloviev and Siklos[26] and the results of the nuclear reaction studies,[31] lead to the following preferences for configurations of the 4 –, 5 –, and 6 – states: $\{n[734]\,\frac{9}{2}-;\ n[620]\,\frac{1}{2}+\}_{4-}$, $\{n[734]\,\frac{9}{2}-;\ n[620]\,\frac{1}{2}+\}_{5-}$, $\{p[633]\,\frac{7}{2}+;\ p[521]\,\frac{3}{2}-\}_{5-}$, and $\{n[734]\,\frac{9}{2}-;\ n[622]\,\frac{3}{2}+\}_{6-}$. Since only one $K\pi=4-$ and one $K\pi=6-$ band has been identified in the present study we assign the 1255.5-keV band to the $\{n[734]\,\frac{9}{2}-;\ n[620]\,\frac{1}{2}+\}_{4-}$ configuration and the 1499.6-keV state to the $\{n[734]\,\frac{9}{2}-;\ n[622]\,\frac{3}{2}+\}_{6-}$ configuration. Both these assignments are confirmed by the ^{249}Cf(d,p) reaction spectroscopy[31] where several members of these bands are identified and the reaction cross sections are consistent with the above assignments. The logft value of the EC transition to the 6 – state is 6.4 which is higher than the ~5.7 value obtained for the $p[521]\,\frac{3}{2}- \rightarrow n[622]\,\frac{3}{2}+$ transition in ^{251}Es EC decay.[2] The EC transition to the 4 – state at 1255.5 keV involves $\Delta I = \Delta K = 2$ and hence very little EC intensity is expected for this state. This is consistent with the observed EC intensity of $0^{+150}_{-0}\%$.

Of the two $K\pi=5-$ bands, one band should have a $\{n[734]\,\frac{9}{2}-;\ n[620]\,\frac{1}{2}+\}$ assignment. The rotational constant for the 1396.2-keV band is 5.1389 ± 0.0005 keV, which is quite different from the value of 5.5602 ± 0.0005 keV for the 4 – band. If both states were made of the same single-particle components one would expect very similar rotational constants for them. This, then, suggests that the $\{n[734]\,\frac{9}{2}-;\ n[620]\,\frac{1}{2}+\}$ configuration should be assigned to the 1478.5-keV state (rotational constant[34] = 5.7 ± 0.2) and not to the 1396.2-keV band.

From the present radioactive data alone it is not possible to make a definite choice among the two configurations $\{p[633]\,\frac{7}{2}+;\ p[521]\,\frac{3}{2}-\}_{5-}$ or $\{n[734]\,\frac{9}{2}-;\ n[631]\,\frac{1}{2}+\}_{5-}$ for the 1396.2-keV band, although calculations of Soloviev and Siklos[26] prefer the former. The 1396.2-keV band has recently[31] been excited strongly in ^{249}Bk(α,t) proton transfer reaction and is given the $\{p[633]\frac{7}{2}+;p[521]\frac{3}{2}-\}$ assignment. The 1478.5-keV band was populated[31] strongly in the ^{249}Cf(d,p) neutron transfer reaction and was given the $\{n[734]\,\frac{9}{2}-;\ n[620]\,\frac{1}{2}+\}$ assignment. Both the 1396.2- and 1478.5-keV bands were

excited in both the neutron and proton transfer reactions[31] clearly indicating that the two-neutron and two-proton states are mixed. From the ^{249}Cf(d,p) reaction data the cross section ratio $[d\sigma(1396)/d\Omega]/[d\sigma(1478)/d\Omega]$ was found to be 0.234 ± 0.016. The mixing between the two-neutron and two-proton configurations was explained in terms of the residual neutron-proton interaction.[35]

The radioactive data are consistent with the above assignments and mixing of the two $K\pi = 5-$ bands. The strong γ decay of the 1478.5-keV level to the 1396.2-keV state can only occur if the two 5− configurations are mixed; otherwise such a transition would involve change of two particles which is forbidden. The logft value of 6.4 for the EC transition to the 1478.5-keV state is in excellent agreement with the value of 6.2 observed for the $p[521]\frac{3}{2}- \rightarrow n[620]\frac{1}{2}+$ transition in ^{251}Es EC decay.[2] The lower limit of 7.3 on the logft value to the 1396.2-keV state is also in good agreement with the value of 7.1 obtained for the $p[633]\frac{7}{2}+ \rightarrow n[734]\frac{9}{2}-$ transition in ^{249}Bk β^- decay.[21]

G. Rotational constants

The effect of adding another nucleon to an odd-A nucleus (such that there are two unpaired particles) is to increase the moment of inertia of the even-A nucleus. The moment of inertia, $\mathcal{I}$ of a two-quasiparticle band can be calculated[36] by adding the moments of inertia of the constituent states and subtracting that of the even-even core. In the case of the odd-odd nucleus $^{250}_{97}$Bk a satisfactory agreement was obtained[36] between the observed and calculated rotational constants. Using the data on ^{249}Cf (Ref. 7), ^{251}Cf (Ref. 32), and ^{251}Es (Ref. 37) we obtain the following values of rotational constant, $\hbar^2/2\mathcal{I}$, for the two-quasiparticle states of ^{250}Cf: $\{n[734]\frac{9}{2}-;\ n[620]\frac{1}{2}+\}$, 5.29 keV; $\{n[734]\frac{9}{2}-;\ n[622]\frac{3}{2}+\}$, 5.45 keV; $\{p[633]\frac{7}{2}+;\ p[521]\frac{3}{2}-\}$, 4.74 keV. The experimental values for the two-neutron states 1255.5 (4−) and 1478.5 (5−) and two-proton state 1396.2 (5−) are 5.56, 5.7, and 5.1 keV, respectively. It is obvious that the measured values are larger than the calculated values. However, we note that they are very close to the single-particle state values with the lowest $\hbar^2/2\mathcal{I}$; e.g., for the $\frac{9}{2}-[734]$ state $\hbar^2/2\mathcal{I} = 5.68$ keV and for the $\frac{7}{2}+[633]$ state $\hbar^2/2\mathcal{I} = 5.28$ keV.

The authors wish to thank the cyclotron crew for many irradiations, F. Wagner, Jr. for assistance in the data analysis, and R. R. Chasman and A. M. Friedman for helpful discussions.

*Work performed under the auspices of the U. S. Energy Research and Development Administration.

[1]B. G. Harvey, A. Chetham-Strode, Jr., A. Ghiorso, G. R. Choppin, and S. G. Thompson, Phys. Rev. 104, 1315 (1956).
[2]I. Ahmad, R. K. Sjoblom, R. F. Barnes, E. P. Horwitz, and P. R. Fields, Nucl. Phys. A140, 141 (1970).
[3]D. F. Peppard, S. W. Moline, and G. W. Mason, J. Inorg. Nucl. Chem. 4, 344 (1957).
[4]I. Ahmad, R. F. Barnes, R. K. Sjoblom, and P. R. Fields, J. Inorg. Nucl. Chem. 34, 3335 (1972).
[5]G. R. Choppin, B. G. Harvey, and S. G. Thompson, J. Inorg. Nucl. Chem. 2, 66 (1956).
[6]J. Lerner, Nucl. Instrum. Methods 102, 373 (1972).
[7]I. Ahmad, R. K. Sjoblom, and P. R. Fields, Phys. Rev. C 14, 218 (1976).
[8]M. S. Freedman, F. Wagner, F. T. Porter, J. Terandy, and P. P. Day, Nucl. Instrum. Methods 8, 225 (1960).
[9]M. S. Freedman, F. Wagner, F. T. Porter (unpublished).
[10]I. Ahmad and F. Wagner, Nucl. Instrum. Methods 116, 465 (1974).
[11]Evidence of the 2.1-h activity was seen in the conversion lines of the 42.72-keV transition. In addition the K lines of the 1031.8- and 989.0-keV transitions, known to be associated with the 2.1-h decay, were sought and found early in one run. All intensities in Tables I and II are for the 8.6-h isomer.
[12]R. S. Hager and E. C. Seltzer, Nucl. Data A4, 1 (1968).
[13]O. Dragoun, H. C. Pauli, and F. Schmutzler, Nucl. Data A6, 235 (1969); O. Dragoun, Z. Plajner, and F. Schmutzler, Max-Planck-Institute fur Kernphysik, Heidelberg, report No. MPIH-1969-V5 (unpublished).
[14]E. J. McGuire, Phys. Rev. A 3, 1801 (1971).
[15]F. P. Larkins, J. Phys. B 9, 47 (1976).
[16]C. P. Bhalla and D. J. Ramsdale, Z. Phys. 239, 95 (1970).
[17]H. Brysk and M. E. Rose, presented in A. H. Wapstra, G. J. Nijgh, and R. van Lieshout, *Nuclear Spectroscopy Tables* (North-Holland, Amsterdam, 1959), p. 59.
[18]P. Venugopala Rao, M. H. Chen, and B. Crasemann, Phys. Rev. A 5, 997 (1972).
[19]Y. A. Ellis and A. H. Wapstra, Nucl. Data B 3, 76 (1969).
[20]F. Asaro, F. S. Stephens, Jr., S. G. Thompson, and I. Perlman, Phys. Rev. 98, 19 (1955).
[21]S. E. Vandenbosch, H. Diamond, R. K. Sjoblom, and P. R. Fields, Phys. Rev. 115, 115 (1959).
[22]A. Bohr and B. R. Mottelson, K. Dan. Vidensk. Selsk. Mat.−Fys. Medd. 27, No. 16 (1953).
[23]I. Ahmad, Lawrence Radiation Laboratory Report No. UCRL-16888, 1966 (unpublished).
[24]I. Ahmad, A. M. Friedman, R. F. Barnes, R. K. Sjoblom, J. Milsted, and P. R. Fields, Phys. Rev. 164, 1537 (1967).
[25]L. Goodman, H. Diamond, and H. E. Stanton, Phys. Rev. A 11, 499 (1975).
[26]V. G. Soloviev and T. Siklos, Nucl. Phys. 59, 145 (1964).
[27]A. Bohr and B. R. Mottelson, At. Energ. (USSR) 14,

41 (1963) [Sov. At. Energy 14, 36 (1963)].
[28]O. Nathan and S. G. Nilsson, in *Alpha-, Beta- and Gamma-ray Spectroscopy* (North-Holland, Amsterdam, 1965), p. 656.
[29]S. Bjørnholm, J. Borggreen, B. Davies, N. J. S. Hansen, and J. Pederson, Nucl. Phys. A118, 261 (1968).
[30]R. A. Meyer, R. W. Lougheed, J. E. Evans, and R. W. Hoff, Bull. Am. Phys. Soc. 17, 464 (1972); R. A. Meyer (private communication).
[31]S. W. Yates, I. Ahmad, A. M. Friedman, K. Katori, C. Castaneda, and T. E. Ward, Phys. Rev. Lett. 36, 1125 (1976).
[32]I. Ahmad, F. T. Porter, M. S. Freedman, R. F. Barnes, R. K. Sjoblom, F. Wagner, Jr., J. Milsted, and P. R. Fields, Phys. Rev. C 3, 390 (1971).
[33]I. Ahmad and J. Milsted, Nucl. Phys. A239, 1 (1975).
[34]K. Katori, A. M. Friedman, S. W. Yates, and I. Ahmad (unpublished).
[35]H. Massman, J. O. Rasmussen, T. E. Ward, P. E. Haustein, and F. E. Bernthal, Phys. Rev. C 9, 2312 (1974).
[36]Wm. C. McHarris, F. S. Stephens, F. Asaro, and I. Perlman, Phys. Rev. 144, 1031 (1966).
[37]I. Ahmad and R. K. Sjoblom (unpublished).